Coordinated Control Strategy of Flexible HVDC Transmission based on New Energy Grid Connection

Yuhong Wang[1], Guoyi Lu[2]

[1]Faculty of Electrical and Control Engineering, Liaoning Technical University, Liaoning,China

[2]Faculty of Electrical and Control Engineering, Liaoning Technical University, Liaoning,China

Abstract

n order to improve the quality of photovoltaic power injected into the grid, a high-voltage flexible direct current (Voltage Source Converter-High Voltage Direct Curren, VSC-HVDC) grid-connected scheme based on a micro-synchronous phasor measurement unit (μPMU) coordinated control strategy is proposed. The four-terminal topology of photovoltaic power plants connected to the grid via VSC-HVDC is designed, and two photovoltaic power plants are connected to the grid via VSC-HVDC model using Matlab/Simulink simulation software to simulate when the light intensity is changed, the photovoltaic power plant is out of operation and the grid voltage occurs In the case of sudden changes, the system voltage, power, and AC side frequency can still maintain stable operation, which verifies the feasibility and effectiveness of the transmission scheme, and improves the stability and power quality of the power grid.

Keywords:Photovoltaic power generation; VSC-HVDC; constant AC voltage control; DC voltage control; PQ control

1 INTRODUCTION

As photovoltaic power generation technology getting mature, the installed capacity of photovoltaic power generation in China is increasing. However, photovoltaic power generation is vulnerable to the influence of external environment, such as light and temperature, which leads to intermittent and fluctuating of active power in the power system; high occupancy ratio brings many impacts on power system, such as the fluctuation of grid voltage、power flow and harmonics which impact on power quality; the poor frequency regulation increases the risk of overfrequency; the high peak output, small electricity quantity and high cost of full consumption of the power.

About the transmission mode of photovoltaic power, the local grid connection mode is mostly used at present, but the local grid is difficult to accept a large number of photovoltaic power, direct grid connection will have a huge impact on the power flow and seriously affect on the power quality.Flexible HVDC transmission technology based on VSC can realize independent control of active and reactive power , asynchronous grid connection, DC transmission and distribution of urban power, power supply to island, flexible control, large transmission capacity and long transmission distance, etc., which plays a significant role in the grid connection of new energy.In this paper, a scheme of grid connected photovoltaic power station via VSC-HVDC is designed，to realizelong-distance transmission of photovoltaic power. An improved coordinated control strategy based on micro synchronous phasor measurement unit (μPMU) is proposed,when the active power and DC voltage of the system fluctuate, the system can automatically adjust to reach the balance state again, so that the system can maintain stable operation and improve the power quality of grid connection.

2 SYSTEM STRUCTURE DIAGRAM OF PHOTOVOLTAIC GRID CONNERCTION THROUGH FLEXIBLE DC

2.1 System topology

Figure 1 shows the topology structure of photovoltaic power station connected to grid through flexible DC transmission system. The system includes two photovoltaic power stations, two rectifier stations at photovoltaic side (vsc1, vsc2) and two inverter stations (vsc3, vsc4). Two photovoltaic power stations are connected in parallel to collect electric energy, connected to vsc1 and vsc2 and transmitted to vsc3 and vsc4 terminals, the power is distributed to each receiving-end grid and load through control strategy.
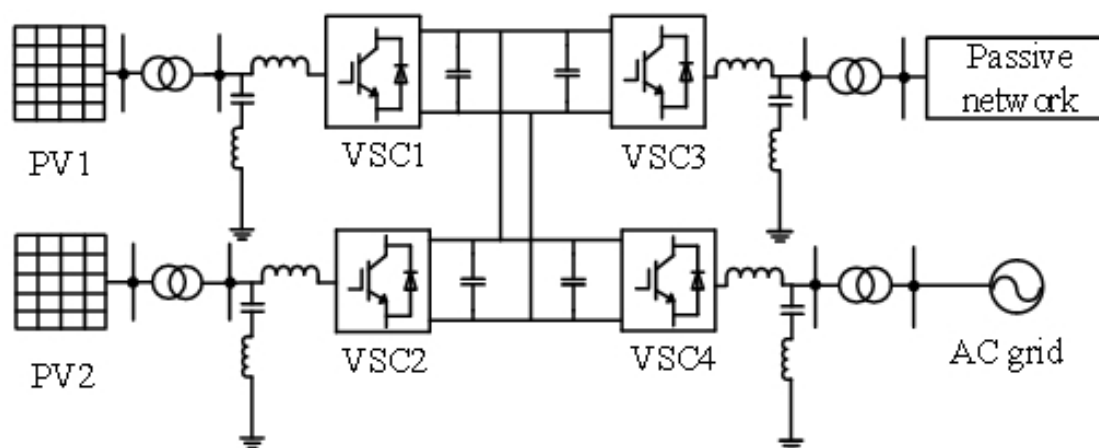

Figure 1. VSC-HVDC system grid-connected topology

2.2VSC system structure and mathematical model
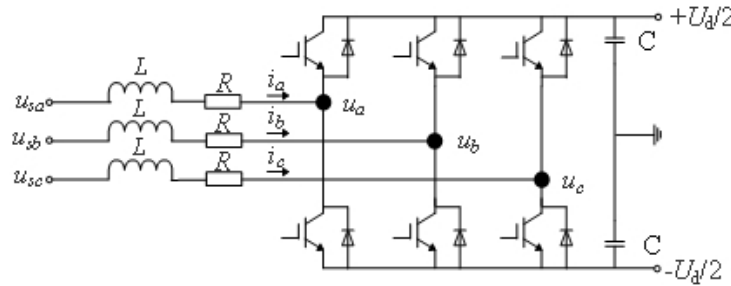
Figure 2 shows the VSC system structure.

Figure 2. Inverter system structure

The two-level topology consists of six arms, each of which consists of IGBT and diode in reverse parallel. According to Kirchhoff's law, the mathematical model of HVDC system can be established in three-phase static coordinate system ABC :

$$L\frac{d}{dt}\begin{pmatrix} i_a \\ i_b \\ i_c \end{pmatrix} = -R\begin{pmatrix} i_a \\ i_b \\ i_c \end{pmatrix} + \begin{pmatrix} u_{sa}-u_a \\ u_{sb}-u_b \\ u_{sc}-u_c \end{pmatrix} \tag{1}$$

Where: L and R are equivalent reactor and resistance of converter respectively; Usa、Usb、Usc、ia、ib、ic are three-phase voltage and current of power grid respectively; Ua、Ub、Uc are three-phase voltage at input side of converter station. When the power grid is in balance, the equation can be obtained.

$$\begin{pmatrix} u_{sa} \\ u_{sb} \\ u_{sc} \end{pmatrix} = \begin{pmatrix} u_s\cos\omega t \\ u_s\cos(\omega t-120°) \\ u_s\cos(\omega t+120°) \end{pmatrix} \tag{2}$$

The park transform of equation (1) is carried out to obtain the mathematical model of AC side of VSC in synchronous rotating coordinates. The park transformation matrix P and its inverse matrix P-1 are as follows:

$$P = \frac{2}{3}\begin{bmatrix} \cos\theta & \cos(\theta-120°) & \cos(\theta+120°) \\ \sin\theta & \sin(\theta-120°) & \sin(\theta+120°) \\ \frac{1}{2} & \frac{1}{2} & \frac{1}{2} \end{bmatrix} \tag{3}$$

$$P^{-1} = \begin{bmatrix} \cos\theta & \sin\theta & 1 \\ \cos(\theta-120°) & \sin(\theta-120°) & 1 \\ \cos(\theta+120°) & \sin(\theta+120°) & 1 \end{bmatrix} \tag{4}$$

Where: θ is the angle between d-axis and a-axis. Substituting equations (3) and (4) into equation (1) shows that:

$$\begin{cases} u_d = -L\dfrac{di_d}{dt} - Ri_d + \omega Li_q + u_{sd} \\ u_q = -L\dfrac{di_q}{dt} - Ri_q - \omega Li_d + u_{sq} \end{cases} \tag{5}$$

Where: u_{sd}、u_{sq} are d-q axis components of grid voltage u_{sabc}, u_d、u_q are d-q axis components of VSC AC side voltage u_{abc} .The control equations of u_d、u_q can be obtained by using feedforward compensation decoupling control strategy.

$$\begin{cases} u_d = -\left[k_p(i_{dref} - i_d) + k_i\int(i_{dref} - i_d)dt\right] + \omega Li_q + u_{sd} \\ u_q = -\left[k_p(i_{qref} - i_q) + k_i\int(i_{qref} - i_q)dt\right] - \omega Li_d + u_{sq} \end{cases} \tag{6}$$

Where k_p、k_i are proportional integral coefficients of d-axis and q-axis respectively. From equation (6), the inner loop decoupling controller based on d-q synchronous rotation coordinate can be obtained as shown in Figure 3.
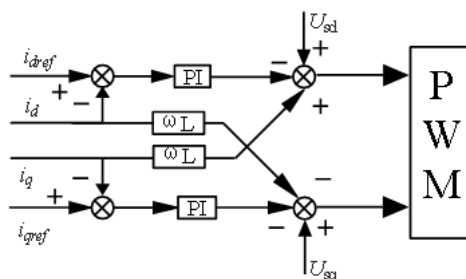

Figure 3. Inner loop current decoupling control

In the coordinate system of synchronous rotating , the instantaneous active power P and reactive power Q absorbed by the converter are respectively:

$$\begin{cases} P = \dfrac{3}{2}\left(u_{sd}i_d + u_{sq}i_q\right) \\ Q = \dfrac{3}{2}\left(u_{sd}i_q - u_{sq}i_d\right) \end{cases} \tag{7}$$

When the grid voltage is oriented to the d-axis in the coordinate system of synchronous rotating , $u_{sd} = u_s$, $u_{sq} = 0$, then the active and reactive power input by the grid to VSC are as follows:

$$\begin{cases} P = \dfrac{3}{2}u_{sd}i_d \\ Q = \dfrac{3}{2}u_{sd}i_q \end{cases} \tag{8}$$

It can be seen from equation (8) that active power and reactive power can be controlled respectively by controlling ID and IQ to realize decoupling control.

3 COORDINATED CONTROL STRATEGY

3.1 Analysis of VSC operation characteristics

Figure 4 is a diagram of VSC-HVDC. U_s、 U_c re the fundamental component of AC bus voltage and VSC input voltage respectively. i is the fundamental current of VSC input P_s、 Q_s are the active and reactive power of AC system input. P_c、Q_c are the active and reactive power of VSC input. P_{dc}、 I_{dc}、 U_{dc} are the active power of DC system, DC line current and DC system voltage respectively .
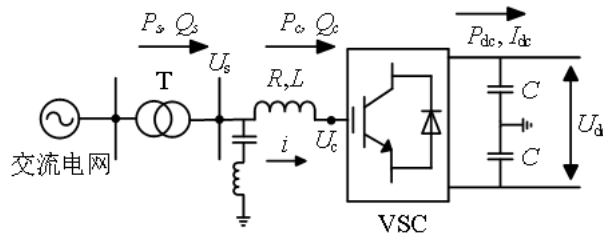

Figure 4. VSC-HVDC diagram

When the VSC at the rectifier side works normally, its input side can be equivalent to a voltage source, and the equivalent circuit is shown in Figure 5.
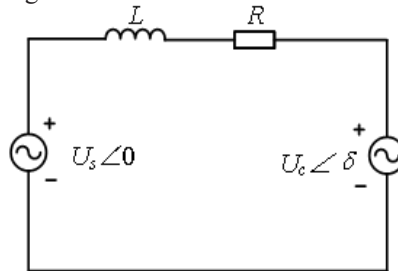

Figure 5. VSCAC side equivalent circuit

Ignoring the commutation reactance and the equivalent loss resistance in VSC, the formula (9) can be obtained：

$$\begin{cases} P_s = \dfrac{U_s \cdot U_c}{X} \sin \delta \\ Q_s = \dfrac{U_s \cdot (U_c \cos \delta - U_s)}{X} \end{cases} \tag{9}$$

δ is the phase angle difference between Us and Uc. Because the power angle difference δ is very small, it can be approximately regarded as $\sin \delta = \delta$, $\cos \delta = 1$, from equation (9), the active power angle droop control formula can be obtained:

$$X^* = \delta_{ref} - \delta_0 + k(P_{ref} - P) \tag{10}$$

Where: k is the droop coefficient, δ_{ref}、$\delta 0$ are the given reference value of phase angle and steady-state operation value P_s ectively, and Pref and P are the given value of power and the actual measured value of power.

According to equation (9), the magnitude and direction of reactive power Q_s can be directly controlled by controlling the amplitude and phase of U_c; the magnitude and direction of active power are determined by power angle δ.When δ > 0, VSC works in rectification state and absorbs active power from AC power grid;

when δ < 0, VSC works in inverter state and outputs power to AC system, and the magnitude and direction of active power can be controlled by changing phase angle δ PWM technology can control modulation ratio M and phase angle δ at the same time, so VSC can control active power and reactive power respectively. By adopting reasonable control mode at each end of converter station, the system can maintain stable operation. Fig. 6 shows the fundamental wave vector diagram of VSC in steady state operation.
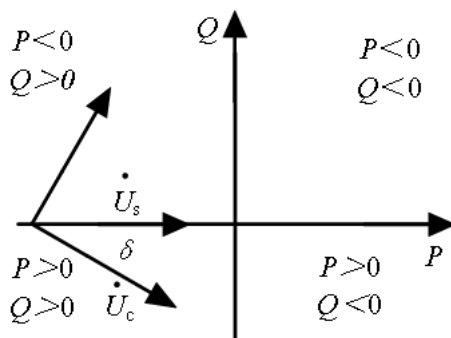

Figure 6. VSC fundamental wave vector diagram

3.2 Coordinated control strategy
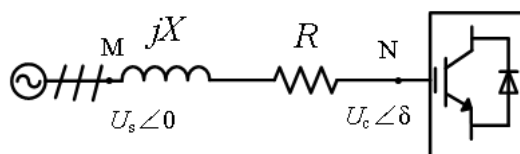
Figure 7 can be obtained by simplifying Figure 4.

Figure 7. VSC-HVDC equivalent structure diagram

Since the amplitude of power angle difference δ is small, a micro synchronous vector measurement unit (μPMU) is introduced to measure power angle δ. μPMU can be used for real-time measurement of power system voltage and current phase of transmission line. the time accuracy of measurement is high, reaching microsecond level. The measurement data is transmitted to δ controller through global positioning system (GPS) or Beidou unified time, the output of active power of the system is precisely regulated by δ to keep the system stability.

The indirectness and randomness of photovoltaic power generation bring great fluctuation to the DC voltage and power of the system, in order to ensure the stable operation of the system and improve the transmission quality, an improved coordinated control strategy based on micro synchronous phasor measurement unit is proposed. As shown in Figure 8, the control structure of photovoltaic power station side is shown.
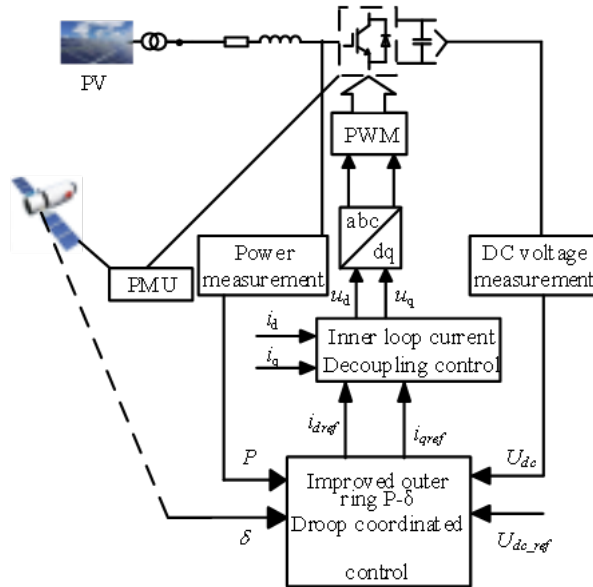
Figure 8. Improved station control structure diagram

Referring to the idea of margin control, the outer loop voltage controller is designed as shown in Figure 9.
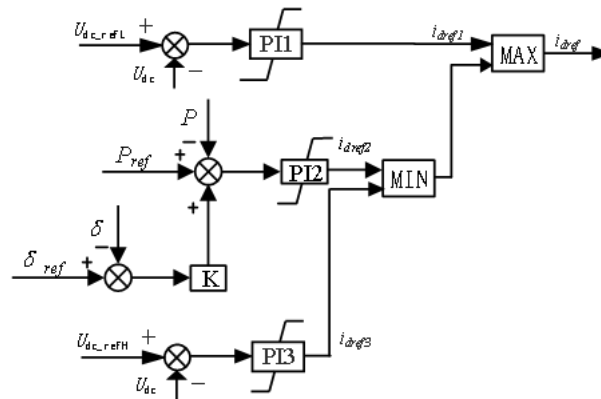

Figure 9. Improve the structure diagram of outer loop control principle

In the figure, U_{dc_refH}、U_{dc_refL} is the given maximum and minimum reference value of DC voltage, PI1、PI3 are the low-order and high-order regulators of DC voltage, PI2 is the p -δ droop control regulator, i_{dref1}、i_{dref2}、i_{dref3} are the output values of PI1、PI2、PI3 respectively.

PI2 control mode is designed

$$i_{dref2} = \left[K_p \left(\delta_{ref} - \delta \right) + K_i \int \left(\delta_{ref} - \delta \right) dt \right] \tag{11}$$

Where: K_p 、K_i are the proportional and integral coefficients of PI2 controller respectively. In Figure 7, at point N, μPMU measures δ in real time and transmits the data to the signal receiver at converter station side to calculate Δδ.The power is obtained by measuring voltage and current, and X* is calculated by droop formula (10). Δδ and ΔP are input to PI2 controller to obtain d-axis reference value Idref of inner loop current, and then PWM reference value is obtained Voltage, generate trigger pulse to PWM modulation, realize DC voltage and power regulation.

In order to ensure the stable operation of the system under extreme environmental conditions, it can be switched to constant DC voltage control according to the fluctuation of the system. The output of each PI controller meets the following requirements:

$$\begin{cases} i_{dref1} = i_{d\,min} \leq i_{dref2} \\ i_{dref3} = i_{d\,max} \geq i_{dref2} \end{cases} \qquad (12)$$

The logical relationship is as follows:

$$i_{dref} = max\left[i_{dref1}, min\left(i_{dref2}, i_{dref3}\right)\right] \qquad (13)$$

According to equation (13), when the converter station is in normal operation, the output   of the controller is determined by i_{dref2}, i.e. $i_{dref} = i_{dref2}$, and the output of vsc1 and vsc2 station controllers in normal operation is determined by P-δ droop controller. According to the droop coefficient, when the photovoltaic active power output fluctuates, the phase angle δ will change. Through the droop curve, the VSC power i_{dref} cted into the DC system is changed to keep the system running stably. The P-δ characteristic curve is shown in Figure 10.
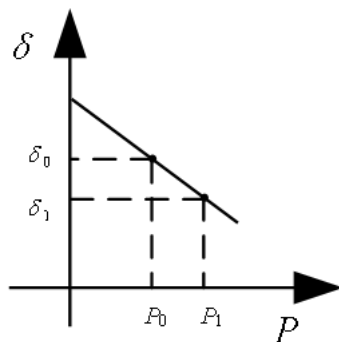

Figure 10. P-δ characteristic curve

During normal operation, the VSC of converter station can fluctuate in a small amplitude in the droop characteristic region. The DC voltage fluctuation will be generated by the charging and discharging of the DC side capacitor in the converter station, and the actual voltage deviation value reaches the preset value. If the VSC works in the p-δ droop control mode, the whole DC system has power excess or shortage, and the DC voltage of the system rises or decreases continuously, and the power variation Δ P and The relationship between the change of DC voltage Δ u is shown in equation (14). The power balance of the system can be stabilized by adjusting the DC voltage.

When a fault occurs on the grid side, in order to realize the low voltage ride through, the DC transmission system reduces the power delivered to the AC grid, resulting in the accumulation of success rate and the increase of DC voltage. At this time, vsc4 station switches to the current limiting control mode to realize self-protection.

The inner loop controller of each converter station adopts feedforward compensation decoupling control in Figure 3 to realize the control of PWM. Table 1 is the switching table of coordinated operation of each end.

Table1. Coordinated control operation switching table of each station

Terminal	Coordinated operation mode		
	$U_{dc} \leq U_{dc\_min}$	$U_{dc\_min} \leq U_{dc} \leq U_{dc\_max}$	$U_{dc} \geq U_{dc\_max}$
VSC1	Constant DC voltage control	$P\text{-}\delta$ droop control	Constant DC voltage control
VSC2	Constant DC voltage control	$P\text{-}\delta$ droop control	Constant DC voltage control
VSC3	PQ control	PQ control	PQ control
VSC4	Current limiting mode	Constant DC voltage control	Current limiting mode

4 SIMULATION ANALYSIS

4.1 Control structure diagram of system

According to the control strategy of each end, the control principle structure diagram can be summarized, as shown in Figure 13. Phase locked loop (PLL) provides reference phase for trigger generation and voltage vector control. The outer loop voltage controller compares the actual measured value with the given reference value, and enters the inner loop circuit after PI regulation to realize the control of DC voltage and active power.
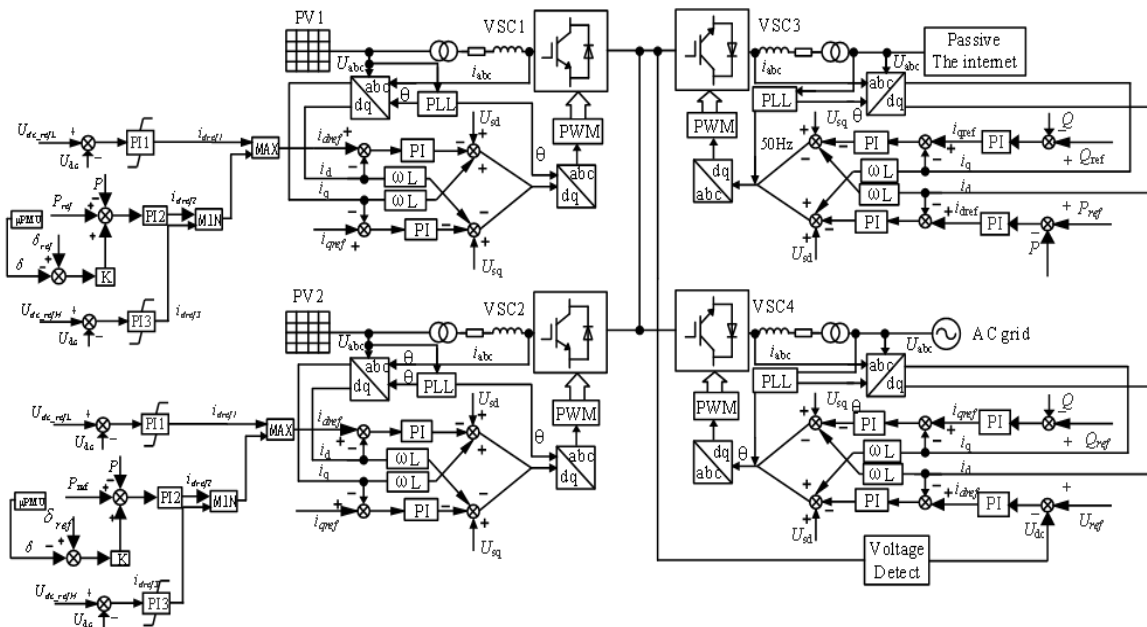

Figure 11. Control system structure diagram

In Matlab / Simulink simulation software, a four terminal transmission system model of photovoltaic power station connected to grid via flexible DC transmission is built. MPPT control is adopted in two photovoltaic power stations to keep the maximum active power output. The DC voltage, power and AC side frequency of the system under three conditions are simulated by setting the initial light intensity S = 800 W/m² and temperature T = 25 °C.

4.2 Simulation results and analysis

Condition 1: set PV power station 1 to increase from initial light intensity S=800 W/m² to S=1000 W/m² at 0.8s, and quit operation at 2s; set PV station 2 to decrease from initial light intensity S=800 W/m² to S=200 W/m² at 1.4s. It can be seen from Figure 12 that at 0.8s and 1.4s, the DC voltage and frequency of the system have a small amplitude fluctuation, lasting for about 0.1s; compared with the traditional control, the fluctuation amplitude of DC voltage is greatly reduced. The active power output of photovoltaic power station 1 increases from 1.5MW to 1.875MW in 0.8s, and decreases from 0.5MW to 0.125MW in 1.4s. The total active power output of the system changes from 2MW-2.375MW-2MW The passive network always absorbs 0.4MW from the DC system. The power variation of the grid connected system is 1.6MW-1.975MW-1.6MW. The DC voltage, power and frequency of the system can reach stable operation quickly.

In 2s, the active power output of photovoltaic power station 1 drops to 0, the total photovoltaic power generation is reduced from 2MW to 0.125MW, the grid connected power of the system is reduced from 1.6MW to -0.275MW, the passive network always absorbs 0.4mw from the DC system; the DC voltage of the system decreases slightly in 2s, the amplitude is within the allowable deviation range, and the duration is about 0.1s, which is more volatile than the traditional control coordination control The simulation results show that the system can still keep stable operation when the active power output of PV system changes and one end of PV system is out of operation.
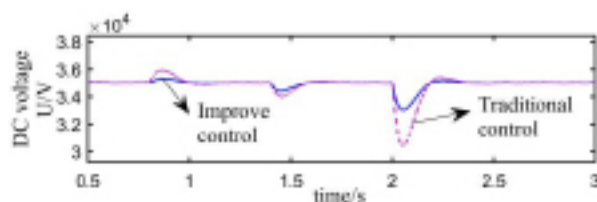
(a) DC voltage waveform
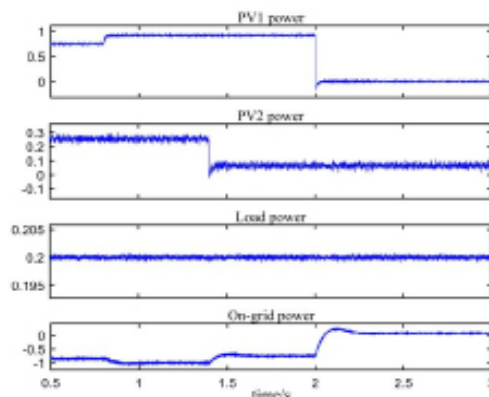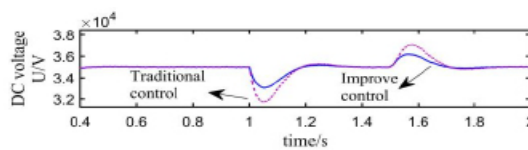

(b) Power waveform at each end
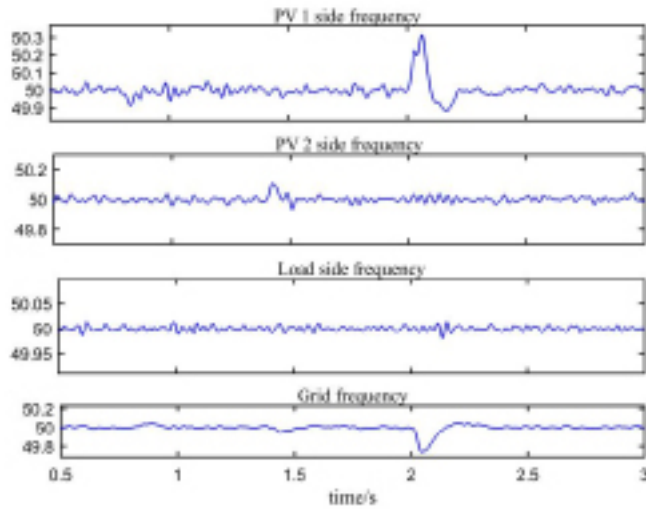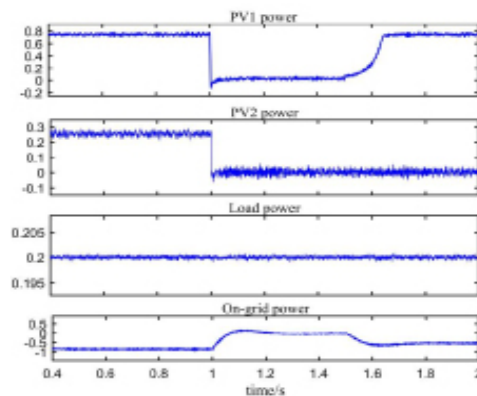
(c) Frequency waveform of AC side at each end

Figure 12. Change the light intensity and exit the running system simulation waveform at one end

Condition 2: two photovoltaic power stations are set to be out of operation in 1s, and then power supply to DC system is restored in 1.5s. Compared with the traditional control system, the active power of the PV system decreases from - 0.4MW to - 1.5MW, and the voltage fluctuation of the PV system decreases from - 0.4MW to - 1.5MW When the frequency of the side and the grid side fluctuates greatly in 1s, the amplitude is within the allowable frequency deviation, and the duration is about 0.1s.

In 1.5s, the power plant 1 resumed to transmit power to the DC system, and the transient transition time was about 0.15s. The power grid gradually recovered to absorb power from the DC system, and the passive network began to supply power from the photovoltaic power station. The DC voltage and frequency at each end fluctuated slightly for 0.05s. The simulation results show that the DC system can still be maintained by the AC power grid when all photovoltaic power stations are out of operation function.

(a) DC voltage waveform
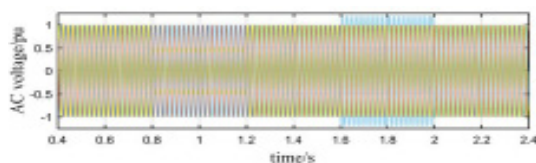

(b) Power waveform at each end
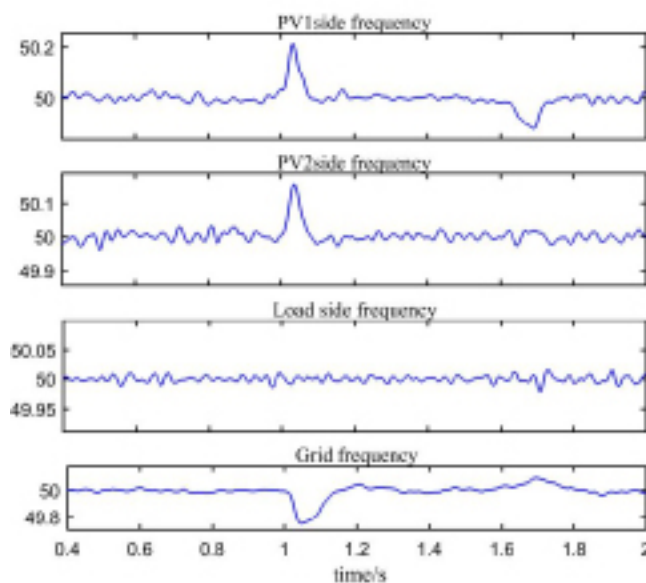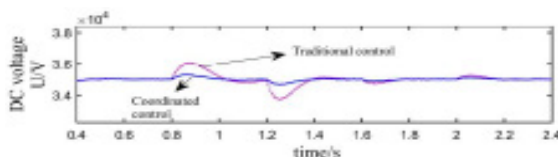
(c) Frequency waveform of AC side at each end

Figure 13. Simulation waveform diagram of the system when all photovoltaic power plants are out of operation

Condition 3: set at 0.8 ~ 1.2s, the voltage of phase a of power grid drops to 50%, and it can be seen from Figure 14 that the voltage of phase a drops to 50% instantaneously in 0.8s, and the DC voltage of the system basically does not fluctuate and keeps stable operation. In 0.8s and 1.2s, the grid connected power fluctuates slightly, and the output power of the PV Plant remains unchanged within the allowable margin. The frequency of power grid side is almost unaffected and keeps stable operation. In 1.2s, the fault is removed and the system quickly returns to stable operation.

Set the grid voltage of phase B to 1.2U at 1.6 ~ 2s. It can be seen from Figure 14 (a) that the voltage of phase B rises to 1.2 times of the rated voltage at 1.6s. At this time, the DC voltage, grid connected power and grid frequency are almost unaffected and keep stable operation. The simulation results show that the transmission system has certain ability to withstand high and low voltage voltage when the voltage is high or low.
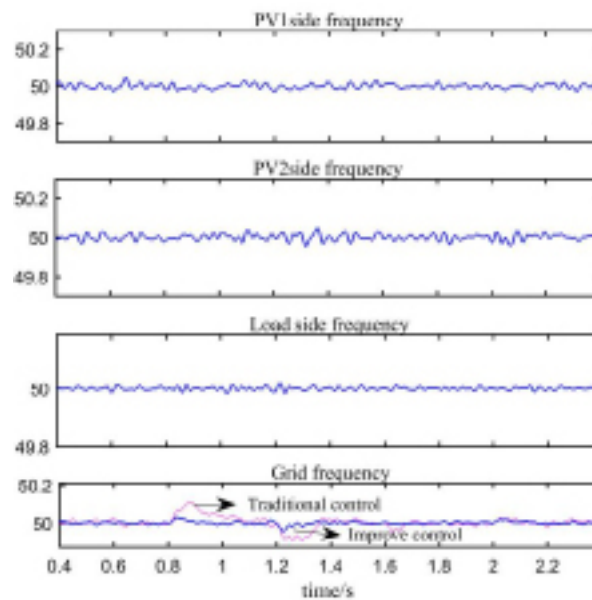

(a)Grid voltage waveform

(b)DC voltage waveform
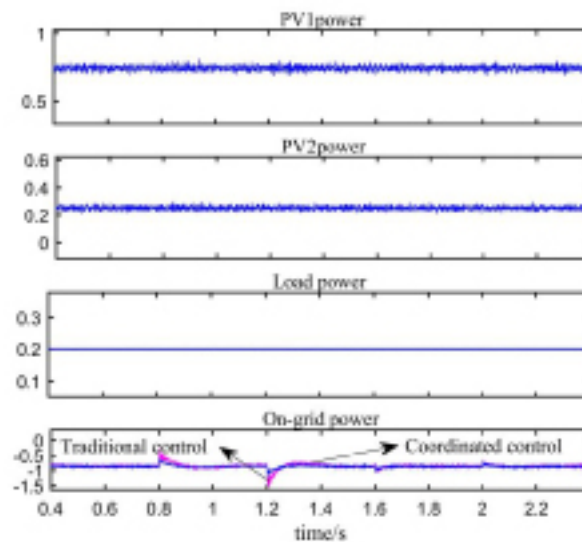
(c)Power waveform at each end

(d)Frequency waveform at each end

Figure 14. The simulation waveform of a three-phase short-circuit fault in the power grid

5 CONCLUSION

Based on the characteristics of photovoltaic power generation and the advantages of coordinated control strategy, this paper studies and analyzes the grid connected system model of two photovoltaic power stations through VSC-HVDC, coordinates the control strategies at each end, and improves the system stability and power quality.

(1) When the light intensity is changed, the active power output of photovoltaic will change. The receiving power station can quickly adjust the absorption of power and reasonably distribute electric energy, so that the power of each end of the system can be balanced and the system can operate stably.

(2) When the photovoltaic system is out of operation, the system voltage and power are basically not affected. The power grid reasonably distributes the absorption of receiving end power, and the fluctuation of DC voltage, power and frequency of each terminal are within the allowable deviation range.

(3) When the grid side voltage fluctuates, the photovoltaic power station can achieve high and low voltage ride through, and can return to normal operation after the grid voltage is stable. It can avoid the oscillation of power flow caused by the shutdown of photovoltaic system due to the transient fault of power grid.

(4) From the point of view of transient process, the system response speed is faster, the fluctuation of grid connected power and DC voltage is reduced, the transient response time is significantly shortened, and the system stability is improved.

(5) From the perspective of AC side frequency, when the power and voltage fluctuate greatly, the AC frequency is almost unaffected, the harmonic is suppressed, and the power quality is improved.

With the continuous increase of photovoltaic power generation, this control strategy provides a theoretical basis for the future access of larger photovoltaic power generation capacity to the grid, and provides a research direction for the control strategy of larger capacity and more complex structure power generation system.

References

Centeno, V., De L. R. J., Thorp, J. S., et al. (2010). Synchronized phasor measurement applications in power systems. IEEE Transactions on Smart Grid, 1(1), 20-27.

Chen, H. (2007). Research on the control and protection strategy of VSC-HVDC system when AC system fails. Zhejiang University. (Doctoral dissertation).

Dianguo, X., Yuchao, L., & Jian, W. (2015). Summary of research on control of multi-terminal HVDC transmission system. Journal of Electrical Engineering and Technology, 30(9), 1-12.

Flourentzou, N., Agelidis, V. G., Demetriades, G. D., et al. (2019). VSC-based HVDC power transmission systems: An overview. IEEE Transactions on Power Electronics, 24(3), 592-602.

Guangfu, T., Luo, X., & Wei, X. (2013). Multi-terminal DC transmission and DC grid technology. Chinese Journal of Electrical Engineering(10), 8-17.

Guanghui, L., Weiran, Z., Guoqing, H., et al. (2012). VSC-HVDC grid-connected topology of photovoltaic power plants and its control strategy. Grid Technology, 36(11), 41-45.

Lei, W., Xiaolong, W., Junxian, H., et al. (2019). Control of photovoltaic grid-connected multi-terminal flexible DC power transmission. Power System Protection and Control, 47(04), 65-72.

Li, Y. (2019). Research on the control strategy of VSC-HVDC transmission system applied to wind power grid connection. Harbin Institute of Technology. (Doctoral dissertation).

Lu, W. X., & Ooi, B. T. (2003). DC overvoltage control during loss of converter in multiterminal voltage-source converter-based HVDC. IEEE Transactions on Power Delivery, 18(3), 915-920.

Majumder, R., Ghosh, A., Ledwich, G., et al. (2009). Angle droop versus frequency droop in a voltage source converter based autonomous microgrid. In IEEE Power & Energy Society General Meeting. IEEE.

Shu, Y., Tang, G., & Pang, H. (2019). Study on Yu'e back-to-back VSC-HVDC system. CSEE Journal of Power and Energy Systems.

Weimin, M., Fangyu, W., Yiming, Y., et al. (2014). Analysis of the status and application prospects of flexible HVDC transmission technology. High Voltage Technology, 40(8), 2429-2439.

Xu, S., Xie, X., & Xin, Y. (2005). Application status and development prospects of wide area measurement system based on synchronous phasor measurement technology. Power System Technology(02), 44-49.

Xu, Y., Wang, S., Wu, X., Wang, J., & Fang, C. (2019). Multi-source collaborative control method of distribution network islands based on synchronous phasor measurement. Power System Technology, 43(03), 872-880.

Xu, Z. (2013). Flexible DC transmission system. China Machinery Industry Press.